

Strain-engineered InAs/GaAs quantum dots for long-wavelength emission

E. C. Le Ru, P. Howe, T. S. Jones, and R. Murray

Centre for Electronic Materials and Devices, Imperial College, London SW7 2BZ, United Kingdom

(Received 19 June 2002; revised manuscript received 11 December 2002; published 3 April 2003)

Using a combination of a seed layer, low-growth rates, and different growth temperatures, we have produced InAs/GaAs quantum dots (QD's) that emit at very long wavelengths (up to $1.39\ \mu\text{m}$ at 293 K) with an ultranarrow inhomogeneous broadening (full width at half maximum of 14 meV at 10 K). The results are discussed in terms of strain relaxation and reduced In/Ga intermixing in the second layer. These two phenomena are interrelated and their control is crucial for achieving long wavelength emission. The QD structures also exhibit interlayer electronic coupling effects. Finally, combining this method with the use of InGaAs in the barrier instead of GaAs, emission wavelengths around $1.5\ \mu\text{m}$ at 293 K have been achieved.

DOI: 10.1103/PhysRevB.67.165303

PACS number(s): 78.67.Hc, 68.65.Hb, 78.55.Cr, 68.37.Ef

InAs/GaAs quantum dots (QD's) are the subject of intense research. The interest is driven primarily by the possibility of growing InAs QD's on GaAs substrates that are optically active at $1.3\ \mu\text{m}$. Alternative technologies for long wavelength emission on GaAs are GaInNAs and GaAsSb QW's.¹ However, owing to the three-dimensional confinement of carriers, QD's are predicted to improve the performances of some devices compared to QW's² and $1.3\ \mu\text{m}$ InAs/GaAs QD lasers with low thresholds have already been demonstrated.^{1,3} However, some problems still need to be overcome to exploit fully the potential of QD's for device applications. A key issue is the relatively low maximum gain that can be obtained from the ground state (g.s.) of a single layer of QD's. This is due in part to the low density of QD's, but also to the large inhomogeneous broadening which means only a subset of the QD ensemble can contribute efficiently to the gain at a given wavelength. Furthermore, extending the wavelength further towards $1.55\ \mu\text{m}$ would also be highly desirable.

One approach to achieve $1.3\ \mu\text{m}$ emission is to reduce the density of QD's, either by using low InAs growth rates,^{4,5} or by alternating submonolayer deposition.³ This results in larger QD's emitting at the correct wavelength with a small full width at half maximum (FWHM), typically 25–30 meV, but the QD density is then low, typically $\approx 10^{10}\ \text{cm}^{-2}$ or less. Alternatively, it has been shown that growing conventional QD's under or within an InGaAs QW can result in a higher density ($3\text{--}4 \times 10^{10}\ \text{cm}^{-2}$) of QD's that emit at $1.3\ \mu\text{m}$.⁶ However, the benefits are in part lost by the larger FWHM ($\geq 35\ \text{meV}$). Moreover, a reduction in the Photoluminescence (PL) efficiency is often observed when InGaAs QW's are used. Combining the two techniques, long wavelength emission ($1.35\ \mu\text{m}$) can be achieved⁷ with a small FWHM (21 meV) but the density remains low. Using growth by metal-organic chemical vapor deposition with high In content InGaAs barriers, emission up to $1.52\ \mu\text{m}$ has been reported but with a strongly reduced PL efficiency.⁸ In all cases, it is also possible to stack several layers of QD's to increase the maximum gain. However, due to the strain interactions between layers, it is not straightforward to obtain closely spaced identical QD layers with optimal properties.^{9,10}

In this paper, we present a method which enables us to grow InAs/GaAs QD's *with only* GaAs in the barrier, emitting up to $\approx 1.4\ \mu\text{m}$ at room temperature, with a reasonable density of $2 \times 10^{10}\ \text{cm}^{-2}$ and an extremely small FWHM (down to 14 meV). The room temperature PL intensity is also improved by a factor of ≈ 5 compared to a standard sample. Our structures consist of two closely spaced QD layers separated by a GaAs spacer layer. The first (seed) layer generates a strain field which extends through the spacer layer,^{11,12} and provides nucleation sites for the second layer QD's, thereby fixing the density. The use of a seed layer has already been demonstrated for high growth rate dots to extend the wavelength to $1.3\ \mu\text{m}$ by increasing the InAs coverage in the second layer.¹³ Here, we grow the second (active) layer of QD's at a low substrate temperature and this results in a large redshift of the QD emission. We also find that the g.s. of the QD's in the first layer is electronically coupled to higher excited states of the dots in the second layer. Using scanning tunneling microscope (STM) and PL characterization, we can attribute the increased emission wavelength to a combination of increased aspect ratio, reduced In/Ga intermixing, and strain relaxation. When using InGaAs in the barrier instead of GaAs, the emission can be extended up to at least $1.48\ \mu\text{m}$.

The QD structures were grown by solid source molecular beam epitaxy (MBE) in a purpose built combined MBE-STM system (DCA Instruments/Omicron GmbH) also equipped with reflection high energy electron diffraction (RHEED). After oxide removal, a $0.5\ \mu\text{m}$ GaAs buffer layer was grown on an epitaxial $n^+\text{GaAs}$ (001) substrate at $580\ ^\circ\text{C}$. The substrate temperature (T_S) was then reduced to $510\ ^\circ\text{C}$ and the samples annealed under an As_2 flux for 10 min. The basic QD structure comprises two layers of InAs/GaAs QD's separated by a GaAs spacer of thickness d . The InAs growth rate was $0.016\ \text{ML/s}$. After deposition of the required amount of InAs for the first layer, the GaAs spacer layer was deposited. T_S was then raised to $580\ ^\circ\text{C}$, the surface annealed for 10 min under an As_2 flux, and T_S reduced again to $480\ ^\circ\text{C}$ or $510\ ^\circ\text{C}$ for growth of the second QD layer. This annealing stage was shown to be important to remove the surface undulation which can have a large effect on the second QD layer properties.^{9,10} Uncapped QD's in the

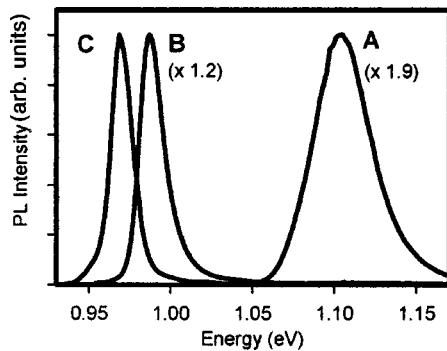


FIG. 1. PL spectra at 10 K from samples A, B, and C. The excitation density is very low ($\approx 0.1 \text{ W cm}^{-2}$) to avoid any emission from the excited states. The PL integrated intensity of the three samples is similar, but the spectra were normalized to their peak intensities to emphasize the reduction of the linewidth and the shift of the emission.

first and second layer were imaged by STM. Constant current STM images were obtained with a sample bias of -3.5 V and tunneling currents of $0.05\text{--}0.2 \text{ nA}$. Samples grown for PL measurements were capped with 40 nm of GaAs before T_S was increased to 580°C for a final GaAs cap of 100 nm . PL measurements were made using an Ar^+ laser for excitation.

Figure 1 shows the low-temperature, low excitation PL spectra of some of the samples studied. Sample A consists of two nominally identical layers formed by deposition of 2.5 ML of InAs at 510°C , and separated by $d = 11 \text{ nm}$ of GaAs. The PL spectrum exhibits one peak centered at 1.10 eV ($1.13 \mu\text{m}$) with a FWHM of 40 meV . At first one might expect that the QD's in the second layer would be more strain-relaxed (lattice constant more InAs-like). This, together with the increased size of the dots in the second layer due to the reduction of the critical thickness (1.4 ML instead of 1.9 ML), should result in a redshift of the PL emission. In previous studies of InAs/GaAs QD bilayers,^{10,14} it was in fact shown that the strain relaxation induces an enhancement of In/Ga intermixing during the capping of the QD's in the second layer, thus compensating the expected redshift. The two QD layers therefore have the same emission energy centered around 1.10 eV .¹⁰ Following this interpretation, long wavelength emission could in principle be obtained if intermixing was prevented or reduced.

Sample B was identical to sample A except that T_S was reduced to 480°C for the growth and capping of the second QD layer. The reduction in the critical thickness was the same as that observed for sample A and is a consequence of the strain field from the dots in the first layer influencing second layer growth.^{10,15} This strain field also forces the dots in the second layer to vertically align with those of the first layer, thus dictating the QD density despite the change in growth temperature. Low-temperature capping was already used on single QD layers to reduce intermixing¹⁶ but it requires a growth interruption, which can affect the QD properties.¹⁷ Here the presence of the seed layer allows both growth and capping (without interruption) of the second layer at a low temperature without a change in density. The

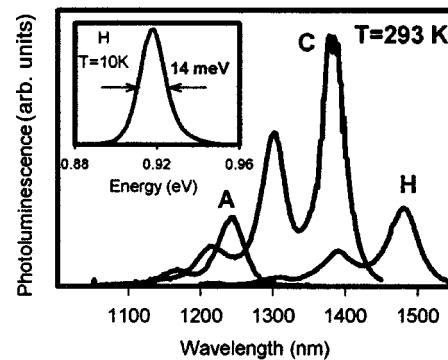


FIG. 2. Comparison of the room temperature (293 K) PL spectra of samples A, C, and H, at an excitation of $\approx 50 \text{ W/cm}^2$. The inset shows the low excitation PL spectrum of sample H at 10 K .

PL spectrum of sample B is remarkably different from that of A (see Fig. 1). The emission from the second QD layer is redshifted by $\approx 120 \text{ meV}$, to 0.988 eV ($1.255 \mu\text{m}$) at 10 K and the FWHM is reduced to 17 meV . Sample C was identical to B except that the InAs coverage in the second layer was increased to 3.2 ML to obtain larger dots and further extend the wavelength.⁵ An additional redshift to 0.970 eV ($1.278 \mu\text{m}$) is observed for the second layer emission, with a FWHM of only 14 meV (see Fig. 1). Another sample was grown identical to C except that the substrate temperature was further reduced to 460°C for growth and capping of the second layer. The emission from this sample is comparable to that of sample C, indicating that intermixing effects are already strongly quenched at a temperature of 480°C .

Figure 2 shows the non-normalized room temperature spectra of some of the samples used for this study. The emission for sample C occurs at $1.39 \mu\text{m}$ at 293 K with an integrated PL intensity ≈ 5 times larger than sample A. This improvement is partly due to the deeper confining potential but nevertheless demonstrates the high emission efficiency of sample C, which would therefore be suitable for applications around $1.4 \mu\text{m}$. Moreover, the emission of the first excited state, where the saturated gain is twice as large as in the ground state owing to the increased degeneracy, is observed at $1.3 \mu\text{m}$. This, together with the reasonable QD density and the narrow FWHM could lead to major improvements for applications at $1.3 \mu\text{m}$ where a large gain is required, such as vertical cavity structures. It is interesting to note in this context that it is possible to stack several such pairs of layers with a separation of 50 nm (not shown here) in order to increase the gain further.

In samples B and C, the GS emission from the first layer around 1.10 eV is not observed at low excitation. This energy is in fact close to that of the second excited state of the QD's in the second layer and these two states are electronically coupled.^{9,18} Using limited-area PL under high excitation,⁹ we confirmed that the first layer does indeed emit around 1.10 eV . This peak is not observed at low excitation however, since carriers captured in the GS of a QD in the first layer tunnel to the second excited state of the vertically aligned dot in the second layer, where they relax rapidly to lower states, resulting in emission from only the second

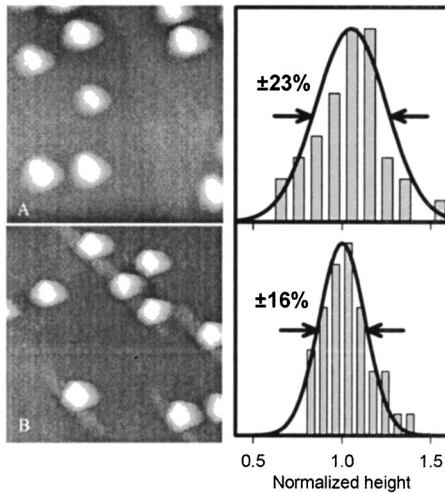


FIG. 3. 200 nm \times 200 nm STM images of uncapped QD's in the second layer of samples A and B. The average QD volume and the density (also measured from larger AFM images) are the same in both samples, despite the difference in growth temperature. The normalized height distribution of each sample, measured from several such STM images, is represented by histograms alongside their respective STM pictures.

layer.⁹ This interpretation was confirmed by growing two samples identical to C but with larger spacer thicknesses of 15 and 18 nm. The emission energy of each QD layer was identical for all three samples, which is therefore ideal for studying the mechanisms of carrier tunneling in asymmetric artificial molecules. A very small emission from the first layer is observed for $d=15$ nm (60 times less intense than the second layer peak), while a much clearer peak is observed for $d=18$ nm (only 4 times less intense than the second layer). This increase with d in the relative intensity of the first layer PL is a clear indication of the reduction of the tunneling rate as the spacer thickness is increased.¹⁸ Following the arguments described in Ref. 9, we can extract a tunneling time of the order of 16 ps for $d=15$ nm and 250 ps for $d=18$ nm.

To complete our interpretation of the observed redshift, STM measurements of the uncapped second layer QD's in samples A and B were performed. Representative images are shown in Fig. 3. The QD density is the same in both cases, as also confirmed by larger (1 $\mu\text{m}\times 1 \mu\text{m}$) AFM scans, and estimated to be $2.0\pm 0.2\times 10^{10} \text{ cm}^{-2}$, which is also the QD density measured from images of the first layer (not shown). However, the reduction of T_S for second layer growth from 510 to 480 $^\circ\text{C}$ would be expected to lead to an increase of the QD density by a factor of around 4.¹⁹ This demonstrates that the strain field from the QD's of the seed layer is strong enough to force QD nucleation only on top of existing dots, thereby dictating the density of the second layer, despite the reduction in the diffusion length of the indium adatoms. The importance of this strain field in QD formation is also evidenced by the reduction of the critical thickness, which is around 1.4 ML for the second layer of both samples as opposed to 1.9 ML in the first.¹⁰ A more quantitative statistical analysis of the STM data is summarized in Table I. The

TABLE I. PL (10 K) and STM data [average area (\bar{A}), height (\bar{h}), and volume (\bar{V})] of the second layer QD's of samples A and B. σ_h is the standard deviation of h .

	PL (μm)	FWHM (meV)	\bar{A} (nm^2)	\bar{h} (\AA)	\bar{V} (10^6 \AA^3)	σ_h (%)
A	1.123	40	721	61.6	2.08	19.7
B	1.255	17	606	69.6	1.97	13.6

normalized height distribution of samples A and B is also shown in Fig. 3 and will be discussed later. The average QD volume is similar for samples A and B. Given that the InAs coverage, the critical thickness and the QD density are also the same, we conclude that the dots have the same composition and that the second layer QD's are close to pure InAs in both samples before capping.¹⁰ It is also apparent from Table I that the average QD height is larger in sample B and, since the average volumes are similar, this means that the QD's in sample B have a higher aspect ratio (defined as height over diameter). The effect of growth temperature on the shape of the dots is difficult to study, since changing the substrate temperature usually results in both a change of the QD density and average volume.¹⁹ In our case, the QD density and volume are fixed owing to the strain field of the first layer, and growth at a lower temperature results in a higher aspect ratio. The increased height in sample B certainly contributes to the observed redshift. However, tall dots could also be grown as single layers and such a long wavelength emission has not been observed. The reduced intermixing due to the low capping temperature and the strain relaxation induced by the presence of the first layer must therefore also play an important role.

To understand these contributions, we studied a series of four samples where T_S for the growth and capping of the second QD layer were varied independently. Using $T_S = 510$ or 480 $^\circ\text{C}$, four samples were grown (C, D, E, and F) whose properties are summarized in Table II. Figure 4 shows the low temperature PL spectra obtained from these samples, where the variations in the PL emission peak are apparent. For samples E and F, a growth interruption (GI) was required to change the temperature before capping, and we verified using samples C and D that such a GI has no effect on the optical properties. When the second layer is grown and

TABLE II. Growth and optical characteristics of samples C to G. Sample G is a single QD layer. For the four other samples, the data refer to the second QD layer.

	T_S (growth)	T_S (cap)	PL (10 K) (μm)	PL (10 K) (eV)	FWHM (meV)
C	480 $^\circ\text{C}$	480 $^\circ\text{C}$	1.278	0.970	14
D	510 $^\circ\text{C}$	510 $^\circ\text{C}$	1.178	1.052	23
E	480 $^\circ\text{C}$	510 $^\circ\text{C}$	1.201	1.032	19
F	510 $^\circ\text{C}$	480 $^\circ\text{C}$	1.210	1.025	23
G	510 $^\circ\text{C}$	480 $^\circ\text{C}$	1.178	1.052	27

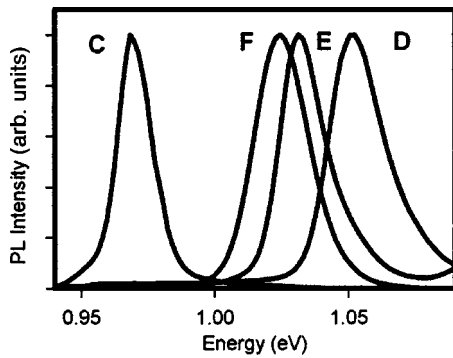


FIG. 4. Low excitation, low-temperature (10 K) normalized PL spectra from samples C to F.

capped at the lowest temperature (sample C), a redshift of 82 meV is observed compared to sample D where the growth and capping are performed at 510 °C. If this redshift was solely due to the *low growth temperature*, we would expect sample E to be identical to sample C, but a redshift of only 20 meV is measured for sample E (with respect to D). Similarly, if the redshift was solely due to the *lower capping temperature*, then sample F would be identical to sample C. Again, although a redshift of 27 meV is observed for F compared to D, it is not as large as the redshift observed for sample C. We conclude that both the growth *and* the capping at a lower temperature contribute to the redshift and that they have different physical origins. From our results, we attribute the first contribution (low temperature growth) to the increased QD height (or aspect ratio), which tends to decrease the confinement energy in the growth direction and leads to the observed redshift in sample E. The second contribution (low temperature cap) is the result of strain and intermixing effects. For sample A we showed that the emission from the second layer was blueshifted due to a larger degree of intermixing during capping because these dots are more strain relaxed.¹⁰ In the second layer of samples D and F, the QD's are identical before capping and more strain relaxed than in a single layer, meaning that they are very sensitive to any strain-induced intermixing. However, if capping is performed at 480 °C (sample F), intermixing is strongly reduced compared to sample D, leading to more indium-rich dots once buried. This explains why the emission from F is redshifted compared to D. Low-temperature capping was shown to result in a small redshift in single layers.¹⁶ Its effect is much more dramatic in our case (QD layer grown above a seed layer) because the strain relaxation in the second layer strongly enhances the intermixing effects.

Moreover, this strain relaxation, if conserved once the dots are buried, is also likely to contribute to the redshift, owing to the strain-induced reduction of the band gap. To confirm this, a single layer of QD's (sample G) was grown under the same conditions as the second QD layer of sample F. Under these conditions, samples F and G have the same dot density and similar average QD volumes. However, the emission of F is redshifted by 27 meV compared to G. Since the capping temperature is low in both cases, intermixing effects are minimized, and the difference can only be attrib-

uted to the strain state of the dots. The strain-relaxed state of the dots in the second layer of sample F is therefore at least partially preserved after capping, resulting in the observed redshift. This series of samples clearly shows that three different mechanisms contribute to the long wavelength emission: larger aspect ratio, reduced intermixing and strain relaxation. When the growth conditions are such that these three mechanisms operate at the same time (sample C), emission up to 1.28 μm at 10 K is obtained, by far the longest wavelength observed from InAs/GaAs QD's when only GaAs is used as the barrier material. Moreover, long wavelength emission is often associated with a decrease in PL intensity due to the use of InGaAs barriers. With this method, long wavelength emission is obtained without the need for InGaAs barriers, and a significant improvement in PL intensity is then obtained.

An additional feature of these structures is the remarkably small inhomogeneous broadening (FWHM of 14 meV). A reduction of the FWHM due to an improved uniformity has previously been observed for stacked QD's.^{13,20} We believe that two other mechanisms operate here to achieve such a narrow linewidth. First, as seen in Table I and Fig. 3, the height fluctuation of the dots in the second layer is smaller when it is grown at a lower temperature and this certainly contributes to the reduction of the FWHM. This effect is also apparent in Table II when comparing the FWHM of samples C and E grown at 480 °C to that of D and F grown at 510 °C. Moreover, it is reasonable to assume that the dots in the ensemble will not all experience the same degree of intermixing during capping, which is then another factor of non-uniformity in the ensemble. It is therefore likely that the reduced intermixing during capping at lower temperatures leads to dots with a more uniform composition, which also contributes to the reduction of the FWHM.¹⁷ This effect is apparent when comparing the FWHM of samples C and E.

Finally, an obvious extension of this study is to try and increase the wavelength further by combining our method with the use of InGaAs layers in the barrier. Figure 2 shows the room temperature, high excitation PL spectrum of sample H, identical to C except that the final 2 nm of the GaAs spacer were replaced by 2 nm of $\text{In}_{0.15}\text{Ga}_{0.85}\text{As}$ and the first 5 nm of the cap of the second layer consisted of $\text{In}_{0.26}\text{Ga}_{0.74}\text{As}$ instead of GaAs. The PL emission peaks at 1.48 μm and extends beyond 1.5 μm . The inset shows the low temperature, low excitation PL spectrum of this sample, where the FWHM is shown to be still very small at 14 meV. The exact explanation of the redshift resulting from InGaAs caps in InAs QD's is still a controversial subject. It has been attributed to reduced confinement energies, reduced intermixing or strain relaxation.⁷ In our case, the intermixing is already strongly quenched when capping with GaAs at 480 °C. The fact that a further redshift is observed when capping with InGaAs indicates that the reduction of the strain and confinement energy rather than of the intermixing effects are the dominant mechanisms. Also apparent in Fig. 2 is the reduction in the PL intensity of sample H compared to C, due to the introduction of a large amount of indium in the barrier. Similar effects are observed when using InGaAs barriers to extend the emission of high growth rate dots towards

1.3 μm .²¹ We believe the optimization of the indium composition and thickness of the InGaAs barriers will improve this intensity, and this is currently under investigation. Despite this reduction, Fig. 2 also shows that sample H exhibits an integrated PL intensity similar to sample A, which did not contain any InGaAs. The difference between sample C and H is therefore due to the exceptional quality of C. Samples C and H demonstrate the potential of this method for the fabrication of QD devices operating at wavelengths beyond 1.4 μm . In addition to applications in telecommunications around 1.55 μm , a wavelength of 1.4 μm , which lies just above the water absorption lines, can have applications in free space optical communications and medical science.

Also, we see in Fig. 2 that the second excited state emission of sample H occurs around 1.3 μm , which could also be used for applications at this wavelength.

To conclude, we have presented a method of growing InAs QD's emitting up to 1.4 μm with GaAs barriers and 1.48 μm with InGaAs barriers, with a FWHM as small as 14 meV. This method utilizes a seed layer to fix the density and induce strain relaxation in the second layer, along with lower growth and capping temperature in the second layer. STM and PL analysis allows us to identify strain relaxation and In/Ga intermixing as the key issues for achieving long wavelength emission. Further optimization of the growth process should open a route for 1.55 μm emitters.

-
- ¹V. M. Ustinov and A. E. Zhukov, *Semicond. Sci. Technol.* **15**, R41 (2000), and references therein.
- ²A. Markus, A. Fiore, J. D. Ganière, U. Oesterle, J. X. Chen, B. Deveaud, M. Ilegems, and H. Riechert, *Appl. Phys. Lett.* **80**, 911 (2002).
- ³D. L. Huffaker, G. Park, Z. Zhou, O. B. Shchekin, and D. G. Deppe, *Appl. Phys. Lett.* **73**, 2564 (1998).
- ⁴R. Murray, D. Childs, S. Malik, P. Siverns, C. Roberts, J.-M. Hartmann, and P. Stavrinou, *Jpn. J. Appl. Phys., Part 1* **38**, 528 (1999).
- ⁵P. B. Joyce, T. J. Krzyzewski, G. R. Bell, T. S. Jones, E. C. Le Ru, and R. Murray, *Phys. Rev. B* **64**, 235317 (2001).
- ⁶V. M. Ustinov, N. A. Maleev, A. E. Zhukov, A. R. Kovsh, A. Yu. Egorov, A. V. Lunev, B. V. Volovik, I. L. Krestinov, Yu. G. Musikhin, N. A. Bert, P. S. Kop'ev, Zh. I. Alferov, N. N. Lendentsov, and D. Bimberg, *Appl. Phys. Lett.* **74**, 2815 (1999).
- ⁷K. Nishi, H. Saito, S. Sugou, and J.-S. Lee, *Appl. Phys. Lett.* **74**, 1111 (1999).
- ⁸J. Tatebayashi, M. Nishioka, and Y. Arakawa, *Appl. Phys. Lett.* **78**, 3469 (2001).
- ⁹E. C. Le Ru, A. J. Bennett, C. Roberts, and R. Murray, *J. Appl. Phys.* **91**, 1365 (2002).
- ¹⁰P. B. Joyce, E. C. Le Ru, T. J. Krzyzewski, G. R. Bell, R. Murray, and T. S. Jones, *Phys. Rev. B* **66**, 075316 (2002).
- ¹¹Q. Xie, A. Madhukar, P. Chen, and N. P. Kobayashi, *Phys. Rev. Lett.* **75**, 2542 (1995).
- ¹²J. Tersoff, C. Teichert, and M. G. Lagally, *Phys. Rev. Lett.* **76**, 1675 (1996).
- ¹³I. Mukhametzhanov, R. Heitz, J. Zeng, P. Chen, and A. Madhukar, *Appl. Phys. Lett.* **73**, 1841 (1998).
- ¹⁴M. O. Lipinski, H. Schuler, O. G. Schmidt, K. Eberl, and N. Y. Jin-Phillipp, *Appl. Phys. Lett.* **77**, 1789 (2000).
- ¹⁵O. G. Schmidt, O. Kienzle, Y. Hao, K. Eberl, and F. Ernst, *Appl. Phys. Lett.* **74**, 1272 (1999).
- ¹⁶O. G. Schmidt, S. Kiravittaya, Y. Nakamura, H. Heidemeyer, R. Songmuang, C. Müller, N. Y. Jin-Phillipp, K. Eberl, H. Wawra, S. Christiansen, H. Gräbeldinger, and H. Schweizer, *Surf. Sci.* **514**, 10 (2002).
- ¹⁷S. Kiravittaya, Y. Nakamura, and O. G. Schmidt, *Physica E* **13**, 224 (2002).
- ¹⁸R. Heitz, I. Mukhametzhanov, P. Chen, and A. Madhukar, *Phys. Rev. B* **58**, R10151 (1998).
- ¹⁹P. B. Joyce, T. J. Krzyzewski, G. R. Bell, B. A. Joyce, and T. S. Jones, *Phys. Rev. B* **58**, R15981 (1998).
- ²⁰H. Heidemeyer, S. Kiravittaya, C. Müller, N. Y. Jin-Phillipp, and O. Schmidt, *Appl. Phys. Lett.* **80**, 1544 (2002).
- ²¹H. Y. Liu, X. D. Wang, J. Wu, B. Xu, Y. Q. Wei, W. H. Jiang, D. Ding, X. L. Ye, F. Lin, J. F. Zhang, J. B. Liang, and Z. G. Wang, *J. Appl. Phys.* **88**, 3392 (2000).